

## Probing the surface of Ganymede by means of bistatic radar with the JUICE mission

Brighi Giancorrado<sup>1,a \*</sup>

<sup>1</sup>Department of Industrial Engineering, Alma Mater Studiorum – University of Bologna, 47121 – Forlì (FC), Italy

<sup>a</sup>giancorrado.brighi@unibo.it

**Keywords:** JUICE, Ganymede, Bistatic Radar, RMS Surface Slope, Dielectric Constant

**Abstract.** Scheduled to get to the Jovian system in 2031, the ESA mission JUICE will explore Jupiter and its icy moons with unprecedented detail. Among other radar systems, the JUICE radio science experiment (3GM) will have the technical capability to probe the uppermost few meters of Ganymede's surface carrying out bistatic observations of the moon. In this work, we present a preliminary assessment of X-band downlink bistatic observations of Ganymede by means of JUICE High Gain Antenna during part of its final orbital phase around the moon. For the chosen time window, terrains between 60° N and 60° S appear to produce detectable echoes under the assumption of Ganymede reflecting as a water-ice rich perfectly conducting sphere. For the future activity of the 3GM experiment, more detailed surveys will be extended to the whole mission, comparing different available antennas and frequency bands, and accounting for the priority of different instruments and scientific objectives.

### Introduction

In the wide framework of radio science experiments, employed for decades to remotely probe celestial bodies' interiors [1] [2] [3], ephemerides [4], rings and atmospheres [5] [6] [7], bistatic radar observations were successfully employed since the end of the sixties to study the surface of planets, satellites and asteroids [8]. When a radio signal is sent to a target body and reflected from its surface, terrain's features with scales proportional to radar wavelengths interact with it. A proper processing of the specular reflection from the planet can provide information about surface roughness in terms of root-mean-square (RMS) slope, near-surface relative dielectric constant and porosity of the target [8].

On its way to launch from the Guiana Space Center in April 2023, the ESA mission JUICE will reach the Jovian system in 2031 to explore the gas giant and its icy moons with unprecedented detail, with a particular emphasis on Ganymede. Among other instruments, the spacecraft will be equipped with the 3GM radio science experiment to address scientific objectives pertaining to gravity, geophysics and atmospheric science through radio tracking and radio occultations [9]. Given the capabilities of 3GM, downlink bistatic radar observations of Ganymede, in both X ( $\lambda \approx 3.6$  cm) and Ka-band ( $\lambda \approx 0.9$  mm), could help constraining the surface composition and near-surface structure of the two major geologic terrain types of the icy moon, i.e. the bright and dark regions [9].

In this work a preliminary assessment of downlink bistatic radar observations of Ganymede by means of JUICE is proposed. The investigation of a short time window is brought as an example, but the same type of analysis can be carried out for any other phase of the mission. Alongside the potential coverage, the main constraints to both feasibility of observation and expected quality of the scientific results are described in details, and supported by some useful, yet simple, analytical formulas.



After a brief introduction to the JUICE mission and its 3GM experiment, an overview of bistatic radar experiment is provided. The opportunity investigation is shown in the final section, followed by some conclusions.

### **The JUICE Mission**

The JUICE (JUper ICy moons Explorer) mission is a large-class interplanetary mission of European Space Agency (ESA) Cosmic Vision 2015-2025 program that will provide the most comprehensive exploration of the Jovian system to address the theme of the emergence of habitable worlds around gas giants [9]. From 2031 to 2035, JUICE will orbit around Jupiter to enforce and deepen our knowledge of the giant gaseous planet and its three icy moons: Europa, Callisto and the prime target of the mission, Ganymede. A mindfully planned synergy between 10 state-of-the-art instruments and the 3GM radio science experiment will undertake a thorough investigation of the chemical composition, structure and evolution of the satellites' surfaces, inner layers and cores, trying to shed some light on the subsurface oceans believed to hide beneath the icy shell of the moons [10].

Scheduled for launch in April 2023, the JUICE orbiter will reach the Jovian system in July 2031 after an 8-year long cruise. Once in orbit around Jupiter, the spacecraft will perform a Jupiter Tour made of 2 flybys of Europa, 9 flybys of Ganymede and 21 flybys of Callisto. From December 2034, the JUICE mission will enter its final 9-month long phase orbiting Ganymede along elliptical (GEO) and circular orbits (GCO): the Ganymede orbital phase [11]. Among other scientific objectives, this orbital phase will give to JUICE the chance of sounding the icy crust of Ganymede to explore for the presence of water and reveal information about the moon's surface structure, origin and evolution. A powerful Ice Penetrating Radar (RIME) will work alongside infrared and ultraviolet spectrometers (MAJIS,UVS), a visible camera (JANUS), a laser altimeter (GALA) and the 3GM experiment to constrain Ganymede's surface properties and geology [9].

The 3GM radio science experiment will rely on the radio link between the on-board radio communication system and Earth stations to retrieve meaningful physical information about space bodies from observables of transmitted radio signals. The nominal investigations that the JUICE orbiter is scheduled to perform by means of 3GM are accurate measurements of the Galilean moons' gravity and radio occultations of neutral atmospheres and ionospheres of Jupiter, Callisto, Europa and Ganymede. Observations of Jupiter's rings physical properties can be carried out as experiments of opportunity, alongside occultations of the Io plasma torus and bistatic radar probing of the surface of the icy moons [9] [12].

### **Bistatic Radar Experiments**

The theory behind quasi-specular bistatic radar (BSR) experiments was developed by Fjeldbo in [12], where he modeled reflections from a rough planet's surface with gaussian statistics using a simplified physical optics model, the Kirchhoff Approximation (KA). Then, he retrieved surface information from the modeled echoes. The planet's surface is assumed to feature i) isotropic and homogeneous behavior, ii) correlation length larger than  $\lambda$  and iii) negligible subsurface scattering [8]. The model was proved to work fairly well for various planetary bodies like the Moon, Mars and Venus [13] [14] [15].

Figure 1 shows a downlink specular near-forward bistatic geometry, where the spacecraft acts as the transmitter and the ground stations on Earth receive echoes from the target planet. In this traditional geometry, chosen for this work, the JUICE orbiter would transmit an unmodulated circularly polarized signal to the target body, Ganymede.

If the planet’s surface satisfies the aforementioned assumptions, the majority of the echoes from

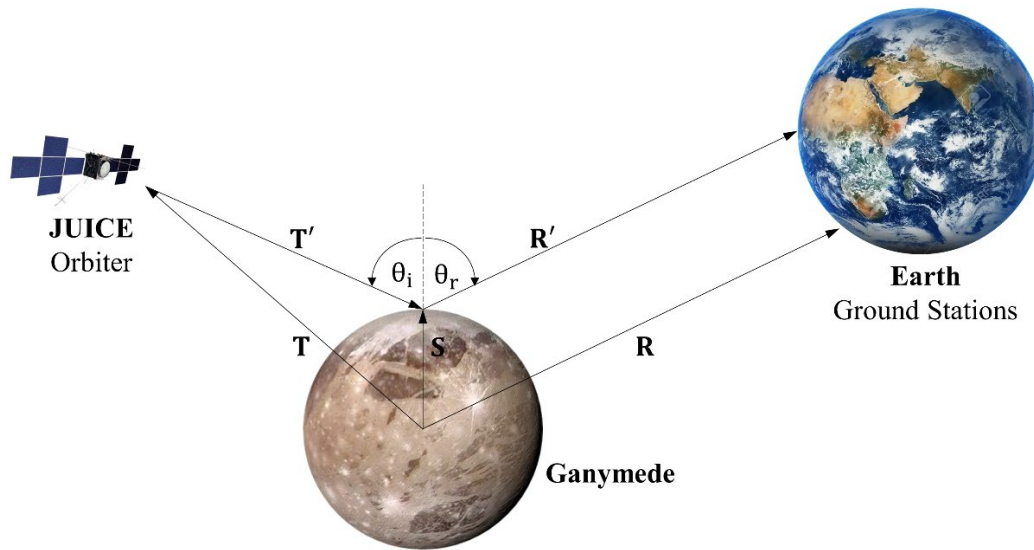


Figure 1 JUICE bistatic observation of Ganymede. Example geometry of a downlink forward specular bistatic radar experiment

the moon are expected to travel in the specular direction ( $\theta_i = \theta_r$  in Figure 1) [8]. If JUICE is pointed towards the moving specular point on Ganymede (S in Figure 1), instantaneously constrained by the relative geometry between JUICE, Ganymede and Earth, echoes will be successfully received on ground. After the reflection, the polarized signal will be broadened in frequency because of surface roughness and will be polarized in both the original (SC) and an orthogonal circular sense (OC) compared to the incoming wave [8].

The differential Doppler between different regions of the reflecting area over the target planet induces the frequency broadening of the echoes. While the distance between transmitter (T) and receiver (R) from the specular point (S) over the target planet are changing, the signal travelling via the specular point undergoes a Doppler shift:

$$f_s = -\frac{1}{\lambda} \frac{d}{dt} \{|T'| + |R'|\}. \tag{1}$$

Differently from Figure 1, in the real world signals transmitted by an antenna travel through solid angles in space. A finite area of Ganymede will be illuminated, and reflections from that can be described, using a physical optics perspective, as a summation of discrete specular contributions arising from variously tilted facets with an effective length-scale of  $\approx 100\lambda$  [8]. The average adirectional tilting of these facets is a measure of surface roughness, and the first output of BSR experiments: the RMS slope.

For a perfectly smooth sphere, the facet where the specular point lies will be the only one contributing to the specular echo. As rougher spheres are considered, facets away from the specular point will be properly tilted to contribute to the overall echo headed to Earth, and their contribution will be Doppler shifted differently from the specular point’s one. As the spatial distribution of these properly oriented reflectors gets broader with roughness, the power spectrum of echoes gets broader in frequency. The spectral broadening can be related to the RMS slope ( $\zeta$ ) with the following formula:

$$B = 4\sqrt{\ln(2)} \left( \frac{V_s \zeta}{\lambda} \right) \cos \theta. \quad (2)$$

Where  $V_s$  is the specular point velocity over the planet's surface,  $\lambda$  is the radar wavelength and  $\theta$  is the incidence angle of observation. With some knowledge of the problem geometry, the RMS slope can be hence obtained from the half-power bandwidth (B) of a received echo [12].

One last remark about the inference of the RMS slope is that for a rougher surface reflectors actively contributing to the overall echo are distributed over a spatially broader area around the specular point. If a fraction of these glints is not illuminated their contributions will not appear in the echo and the roughness will be underestimated. The finiteness of the transmitting antenna FOV introduces an upper bound to the observable RMS slope. If the RMS slope is larger than that, it is said that the observation was carried out in beam-limited conditions [8].

The near-surface relative permittivity can be obtained from the power ratio of the orthogonally polarized components of the received signal. Referring again to Figure 1, if transmitter (T) and receiver (R) performances and positions are known, the reflected power at the receiver can be expressed by the bistatic radar equation:

$$P_R = \frac{P_T G_T}{4\pi|T|^2} \sigma \frac{G_R \lambda^2}{(4\pi|R|)^2}. \quad (3)$$

Where  $P_T$  is the transmitted power,  $G_T$  and  $G_R$  are respectively transmitter and receiver gains, and  $\sigma$  is the planet radar cross section [8]. The latter depends on many unpredictable properties of the reflecting surface, such as the different scattering mechanisms effectively contributing to planet's echoes, the observation's geometry and the surface relative permittivity. The dielectric constant contributes to the radar cross section as a reflectivity, which describes how much power, of the original circularly polarized  $P_T$ , is reflected in the same sense ( $P_{SC}$ ) and in the orthogonal sense ( $P_{OC}$ ) of circular polarization [16]. The relation between relative permittivity and circular polarization reflectivity is described by the Fresnel reflection coefficients [16].

A simple model for the radar cross section of a rough planet is derived in [12] under the KA assumptions. For a generic sense of circular polarization with reflectivity  $\Gamma$ , the radar cross section is taken as follows [13].

$$\sigma = \frac{4\pi|T|^2 R_p \cos \theta}{(R_p \cos \theta + 2|T'|)(R_p + 2|T'| \cos \theta)} * \Gamma. \quad (4)$$

With  $R_p$  radius of the target planet. Combining together equations 3 and 4 it can be observed that the ratio between orthogonally polarized powers equals the ratio between circular polarization reflectivities. If we plug this equality into the expression of the Fresnel reflection coefficients the final expression that links relative permittivity ( $\epsilon$ ) and circular power ratio (CPR) can be written as follows:

$$\epsilon = \sin^2 \theta \left( 1 + \frac{\tan^2 \theta}{\text{CPR}} \right). \quad (5)$$

Hence, the near-surface permittivity of a reflecting surface can be retrieved from the ratio between the power of the two orthogonally polarized components of the surface's echoes [8].

It is not straightforward to associate a specific surface composition to a relative dielectric constant, especially for a body like Ganymede. The icy moon is expected to have a water-ice dominant near-surface composition with various fractions of non-ice contaminants [17] [18]. The relative permittivity of pure water-ice is 3.1, but this value varies with ice porosity, purity and temperature. This adds some complexity to the analysis of BSR observations, and increases the importance of a synergy between radar instruments on board JUICE. If a robust knowledge of the local surface composition is available, various models can be employed to describe the dependence of relative permittivity on porosity or ice purity [8] [19]. The surface porosity, for example, could be retrieved from the difference between the observed relative permittivity and the nominal value of 3.1 for water-ice.

### **JUICE Bistatic Radar Opportunities**

The JUICE orbiter has the technical capabilities to perform downlink specular bistatic observations of Ganymede by means of its 3GM experiment. The spacecraft is equipped with a fixed High Gain Antenna (HGA) and a steerable Medium Gain Antenna (MGA). With the help of an on-board Ultra Stable Oscillator (USO), both the antennas are able to transmit and receive in X- ( $\lambda \approx 3.6$  cm) and Ka-band ( $\lambda \approx 0.9$  mm) [9]. The ground segment for the experiment consists of the 35m diameter stations of the ESTRACK network.

In the following, a preliminary assessment of bistatic observations of Ganymede during the GEO phase using the HGA transmitting in X-band is proposed. Both the feasibility and an expected quality of the scientific outputs are addressed.

Since the employment of JUICE instruments for other experiments is not taken into account, the only constraint to the feasibility of the observation is that the transmitting HGA antenna is capable of tracking the specular point. The specular point exists whenever the spacecraft is not behind Ganymede with respect to Earth, and its velocity over the planet's surface depends on the relative motion of JUICE, Ganymede and Earth. Since the HGA is fixed with the spacecraft, its capability to track the specular point depends on the maximum angular velocity the spacecraft can undergo during the mission. The upper bounds chosen for the analysis were the maximum angular velocity and acceleration that the spacecraft will encounter during the Jupiter Tour [11].

The location of the specular point at a given time instant is uniquely determined by the positions of JUICE, Ganymede and Earth, and was computed solving a nonlinear system of three equations with a strong geometrical meaning [20]. Going back to the labels of Figure 1, the following statements can be made about the specular point **S**:

- 1) It lies over the surface of Ganymede's ellipsoid;
- 2) **T'** and **R'** lie on the same plane;
- 3)  $\theta_I = \theta_R$ .

Once the specular point is located, its velocity and the incidence angle observation can be computed.

In terms of quality of the scientific outputs of BSR, different conclusions can be drawn for different surface properties. The RMS slope can be satisfactorily retrieved as long as echoes are detectable and no beam-limitation occurs. To account for the latter, a maximum observable RMS slope was computed for the transmitting antenna FOV throughout the phase, using the expression of an effective reflecting area increasing with the RMS slope [8].

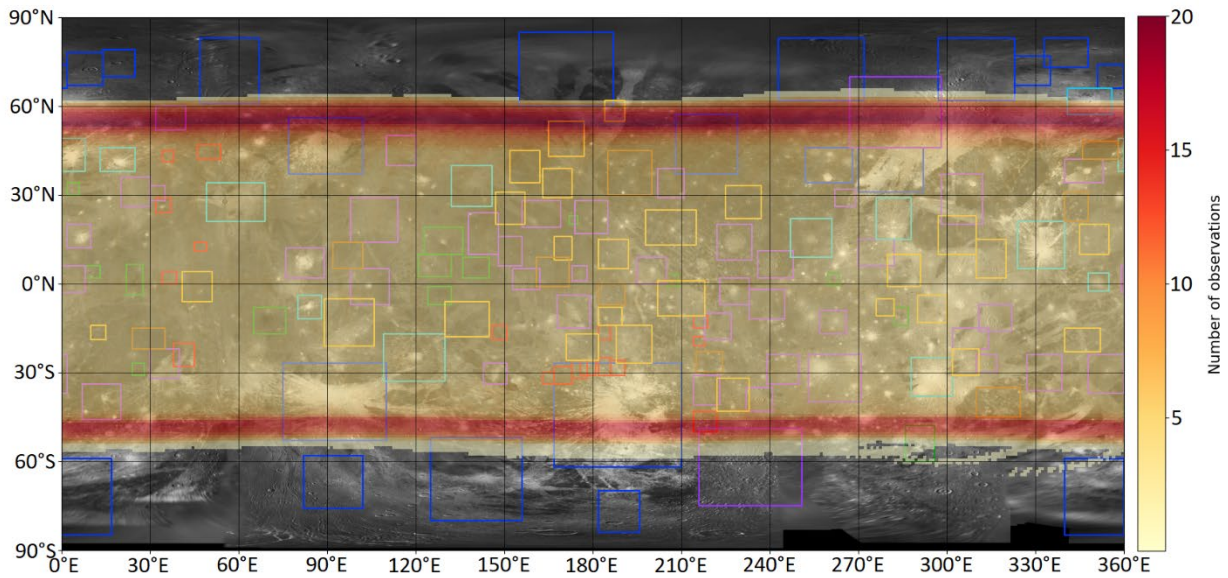


Figure 2 BSR observations coverage during the GEO phase (22/12/34 - 13/05/35). Areas shaded from yellow to red are illuminated by JUICE HGA assuming it to perfectly track the specular point. Different colors relate to a different number of passes over the same region. Colored squares highlight regions of interest over Ganymede according to [10]. Blu: polar deposits; Red: patarae, Green: dark ray craters, Purple: impact craters; Cyan: bright ray craters; Gold: bright terrains; Brown: ancient dark terrain

The dielectric constant can be retrieved from the reflected signals if both the orthogonally polarized components are detectable. For a terrain of known relative permittivity  $\epsilon$ , the Brewster angle is the incidence angle that brings the circular power ratio to unity. If the observation is performed far from the Brewster angle, one of the polarized components will get weak, and its power computation will be more uncertain. For an accurate retrieval of relative permittivity the bistatic observation should be carried out close to the Brewster angle [16]. For a surface relative permittivity to be 3.1, the Brewster angle is roughly  $60^\circ$ .

Figure 2 shows the bistatic radar coverage during the elliptical part of the Ganymede Orbital phase when spacecraft angular velocity and acceleration are below  $0.16^\circ/s$  and  $0.27e-3/s^2$ , and when the incidence angle of observation is between  $50^\circ$  ( $CPR \approx 0.3$ ) and  $70^\circ$  ( $CPR \approx 3$ ). With a time resolution of 60s, the antenna beam pattern of JUICE pointing towards the specular point is plotted.

Assuming a relative permittivity of 3.1 to compute the surface reflectivity and combining equations 3 and 4, the amount of power received on Earth in both polarizations was estimated using the technical parameters shown in Tab. 1. The system noise temperature was assumed to be 28.5 K, which is a nominal value for Malargüe station at elevation of  $50^\circ$ , X-band and clear sky condition [11]. The signal-to-noise ratio (SNR) throughout the phase is always above 22.5 dBHz, which is a satisfying value to see echoes. This result should be considered an upper bound, and does not guarantee echoes will be actually visible, since some of the incoming power may not follow the model of specular reflection proposed by Fjeldbo. Earth-based radar observations of the icy moons hint at the presence of strong subsurface scattering phenomena which would escape Fjeldbo's assumptions, but specular echoes can't be ruled out [17] [22]. As it was the case for other planetary bodies, the validity of the model can be addressed only with new actual observations.

*Table 1 Technical parameters of the bistatic radar radio link between JUICE and 35m Malargüe antenna [11]. \*The power assumed for transmission in X-band is the full power of the Deep Space Transponder (DST)*

	Transmit Power, $P_T$ [W]	Transmit Gain, $G_T$ [dBi]	Receive Gain, $G_R$ [dBi]	Noise Temperature, $T_{sys}$ [K]	Wavelength, $\lambda$ [cm]	Half-power beamwidth, $\theta_{BW}$ [°]
JUICE HGA X-band	52*	43.85	68.2	28.5	3.6	1

**Conclusions**

The JUICE orbiter could be the first spacecraft to carry out BSR observations of one of the icy moons of Jupiter. This experiment would allow for an independent retrieval of surface roughness and relative permittivity which is a very precious return to characterize the surface of the moon, especially looking forward to a synergy with the other on-board radar instruments of the mission.

The purpose of this work was to show how a preliminary assessment of bistatic radar opportunities could be developed for a given mission and target planet. JUICE is taken as an example here, but the same analysis described in this abstract may be applied on other missions. With few simple formulas it was possible to make a case study that provides inputs to discuss when and how it could be better to observe Ganymede by means of bistatic radar.

For the future activity of the 3GM experiment, analogous considerations will be made for the whole mission, comparing the performances of the two antennas at the two possible frequency bands. More advanced considerations should be made about effective maneuverability and availability of the antennas before scheduling these observations. An extended and more detailed version of this analysis could be a starting point to find interesting time windows where BSR observations could be performed with a good expected scientific return.

As a final remark, these remain experiments of opportunity. The final scheduling of these observations will not be solely based on link-budget considerations, but a good compromise should be found between the expected scientific return and the many other scientific objectives of the JUICE mission as a whole: one of the most ambitious space missions of this century.

**References**

[1] M. Zannoni, D. Hemingway, P. Tortora and L. G. Casajus, "The gravity field and interior structure of Dione," *Icarus*, vol. 345, p. 113713, 2020.  
<https://doi.org/10.1016/j.icarus.2020.113713>

[2] L. Gomez Casajus et al., "Gravity Field of Ganymede After the Juno Extended Mission," *Geophysical Research Letters*, vol. 49, no. 24, pp. 1-10, 2022.  
<https://doi.org/10.1029/2022GL099475>

[3] L. Gomez Casajus et al., "Updated Europa gravity field and interior structure from a reanalysis of Galileo tracking data," *Icarus*, vol. 358, p. 114187, 2021.  
<https://doi.org/10.1016/j.icarus.2020.114187>

[4] V. Lainey et al., "Resonance locking in giant planets indicated by the rapid orbital expansion of Titan," *Nature Astronomy*, vol. 4, pp. 1053-1058, 2020. <https://doi.org/10.1038/s41550-020-1120-5>

[5] D. Buccino et al., "Ganymede's Ionosphere Observed by a Dual-Frequency Radio Occultation With Juno," *Geophysical Research Letters*, vol. 49, no. 23, 2022.  
<https://doi.org/10.1029/2022GL098420>

- [6] A. Moirano et al., "Morphology of the Io Plasma Torus From Juno Radio Occultations," *Journal of Geophysical Research: Space Physics*, vol. 126, no. 10, pp. 1-35, 2021.  
<https://doi.org/10.1029/2021JA029190>
- [7] E. Gramigna et al., "Analysis of NASA's DSN Venus Express radio occultation data for year 2014," *Advances in Space Research*, vol. 71, no. 1, pp. 1198-1215, 2023.  
<https://doi.org/10.1016/j.asr.2022.10.070>
- [8] R. A. Simpson, "Spacecraft Studies of Planetary Surfaces Using Bistatic Radar," *IEEE Transactions of Geoscience and Remote Sensing*, pp. 465-482, 1993.  
<https://doi.org/10.1109/36.214923>
- [9] European Space Agency, "ESA JUICE definition study report /Red Book. JUICE Jupiter ICy moons Explorer Exploring the emergence of habitable worlds around gas giants," ESA, 2014.
- [10] K. Stephan et al., "Regions of interest on Ganymede's and Callisto's surfaces as potential targets for ESA's JUICE mission," *Planetary and Space Science*, vol. 208, 15 November 2021.
- [11] A. Boutonnet, A. Rocchi and W. Martens, "JUICE-Jupiter Icy moons Explorer Consolidated Report on Mission Analysis (CReMA)," ESA, 2022.
- [12] G. Fjeldbo, "Bistatic-Radar Methods for Studying Planetary Ionospheres and Surfaces," 1964.
- [13] R. A. Simpson and G. L. Tyler, "Viking Bistatic Radar Experiment: Summary of First-Order Results Emphasizing North Polar Data," *Icarus*, 1981. [https://doi.org/10.1016/0019-1035\(81\)90139-1](https://doi.org/10.1016/0019-1035(81)90139-1)
- [14] L. G. Tyler and H. T. Howard, "Dual-Frequency Bistatic-Radar Investigations of the Moon with Apollos 14 and 15," *Journal of Geophysical Research*, vol. 78, no. 23, pp. 4852-4874, 1973.  
<https://doi.org/10.1029/JB078i023p04852>
- [15] R. A. Simpson et al., "Venus Express bistatic radar: High-Elevation anomalous reflectivity," *Journal of Geophysical Research*, vol. 114, 2009. <https://doi.org/10.1029/2008JE003156>
- [16] R. A. Simpson et al. "Polarization of Bistatic Radar Probing of Planetary Surfaces: Application to Mars Express Data," *Proceedings of the IEEE*, pp. 858-874, 2011.  
<https://doi.org/10.1109/JPROC.2011.2106190>
- [17] B. Hapke, "Coherent Backscatter and the Radar Characteristics of Outer Planet Satellites," *Icarus*, vol. 88, no. 2, pp. 407-417, 1990. [https://doi.org/10.1016/0019-1035\(90\)90091-M](https://doi.org/10.1016/0019-1035(90)90091-M)
- [18] G. J. Black, D. B. Campbell and P. D. Nicholson, "Icy Galilean Satellites: Modeling Radar Reflectivities as a Coherent Backscatter Effect," *Icarus*, vol. 151, no. 2, pp. 167-180, 2001.  
<https://doi.org/10.1006/icar.2001.6616>
- [19] E. Heggy, G. Scabbia, L. Bruzzone and R. T. Pappalardo, "Radar probing of Jovian icy moons: Understanding subsurface water and structure detectability in the JUICE and Europa missions," *Icarus*, vol. 285, pp. 237-251, 2017. <https://doi.org/10.1016/j.icarus.2016.11.039>
- [20] G. Brighi, "Cassini Bistatic Radar Experiments: Preliminary Results on Titan's Polar Regions," *Aerotecnica Missili e Spazio*, vol. 102, pp. 59-76, 2022.  
<https://doi.org/10.1007/s42496-022-00135-4>
- [21] R. A. Simpson, L. G. Tyler and G. G. Schaber, "Viking Bistatic Radar Experiments: Summary of Results in Near-Equatorial Regions," *Journal of Geophysical Research*, vol. 89, no. B12, pp. 10385-10404, November 1984. <https://doi.org/10.1029/JB089iB12p10385>
- [22] R. A. Simpson and G. L. Tyler, "Surface properties of Galilean satellites from bistatic radar experiments," NASA, Washington, Reports of Planetary Geology and Geophysics Program, 1990, 1991.